

zero-CO2 cemeNt ThRough cArBonation of cAlcium Silicates and aluminateS

## **Deliverable D 1.1 Benchmark of Carbonation Reaction Mechanisms of Clinker**

Grant Agreement Nº:	101119715	
Project name:	Zero-CO2 cemeNt ThRough cArBonation of cAlcium Silicates and aluminateS	
Project acronym:	CONTRABASS	
Topic:	HORIZON-MSCA-2022-DN-01-01	
Call (part) identifier:	HORIZON-MSCA-2022-DN-01	
Starting date:	01/01/2024	
Type of action:	HORIZON TMA MSCA Doctoral Networks	
Granting authority:	European Research Executive Agency	
Start date of the project:		
Project duration:	48 months	
Project coordinator:	Hegoi Manzano (UPV/EHU)	

Deliverable No:	D1.1		
Deliverable name:	Benchmark of Carbonation Reaction Mechanisms of Clinker		
WP Nº:	WP1	WP Leader:	Thomas Matschei
Author:	Amal Mathyas		
Contributors:	Amal Mathyas, David Faux, Anh Phan		
Due date:	Month 21	Actual submission date:	September 30, 2025
Dissemination level:	PU		



This project has received funding from the European Union's Horizon Europe research and innovation programme under Grant Agreement No 101119715.

Document history			
Revision	Date	Description	
1	20.08.2025	First draft	
2	07.09.2025	Second draft	
3	10.09.2025	Third draft	
4	11.09.2025	Fourth draft	
5	12.09.2025	Fifth draft	
6	15.09.2025	Final Revision	
7	26.09.2025	WP1 Leader's comment	
8	29.09.2025	Final Version	

Report contributors				
Name	Beneficiary Short	Details of contribution		
	Name			
Amal Mathyas	Surrey	Preparation of 1st draft and revisions		
Anh Phan	Surrey	Preparation of 2nd draft and revisions		
David Faux	Surrey	Preparation of revisions		
Elsa Qoku	RWTH	Final revision		
Thomas Matschei	RWTH	Final revision		

#### Disclaimer

The information in this document is provided "as is", and no guarantee or warranty is given that the information is fit for any particular purpose. The content of this document reflects only the author's view – the European Research Executive Agency (REA) is not responsible for any use that may be made of the information it contains. The users use the information at their sole risk and liability.

The content of this report does not reflect the official opinion of the European Research Executive Agency (REA). Responsibility for the information and views expressed in the report lies entirely with the author(s).



## **Table of Contents**

1.	Executive Summary	5
2.	Abbreviations and acronyms	6
3.	Background	6
4.	Objective/Aim	7
5.	Content of the deliverable	8
5.1. S	imulation Methodology	8
5.1.1.	First-Principles Relaxation of C3S Using Density Functional Theory	8
5.1.2.	Hydration of C3S	9
5.1.3.	Carbonation of C3S	10
5.2. S	ummary of activities and research findings	12
5.2.1.	Analysis of the Structural Properties	12
5.2.2.	Analysis of the Dynamical Properties	13
5.2.3.	Reactivity of CO2-H2O mixture with C3S	15
6.	Conclusions and Future Works	18
7.	References	19

## 1. Executive Summary

Concrete is the foundation of modern infrastructure. The Global Cement and Concrete Association (GCCA) reports that nearly 14 billion cubic meters of concrete are produced worldwide each year, with around 150 tonnes of cement consumed every second (1). In 2019, The Guardian described cement as "the most destructive material on the planet". While journalistic in style, the statement highlights cement's major environmental footprint: its production generates about 8% of global carbon dioxide (CO<sub>2</sub>) emissions and accounts for 7% of industrial energy use, amounting to roughly 4 billion tonnes of CO<sub>2</sub> annually (2). Acknowledging this challenge, the European Green Deal (2020) identified the "decarbonization and modernization of energy-intensive industries such as steel and cement" as a key step toward achieving climate neutrality in the EU by 2050 (1).

The largest share of  $CO_2$  emissions from cement production arises from the calcination of limestone ( $CaCO_3 \rightarrow CaO + CO_2$ ), a chemical reaction that releases more than one ton of  $CO_2$  for every ton of cement produced (3). Since these emissions cannot be fully avoided through plant upgrades alone, reducing the environmental footprint of concrete itself becomes crucial. Among the potential solutions, Carbon Capture and Utilization (CCU) stands out as a promising approach for developing carbon-neutral cement and concrete.

This deliverable investigates the fundamental mechanisms of carbonation curing in tricalcium silicate using Reactive Molecular Dynamics (MD) simulations. Through advanced computational modeling, the study explores the atomic-scale structure, reaction kinetics, and thermodynamic behavior of tricalcium silicate under varying environmental conditions during carbonation. To track the onset of cement carbonation, we analyze the radial distribution function for different atom pairs. The simulation results show that the first radial distribution function peaks for Ca–O<sub>water/Co2</sub> and Ca–C<sub>Co2</sub> occur at 0.24 nm and 0.34 nm, respectively—distances consistent with the structure of calcium carbonate, thereby confirming the formation of carbonation products. In addition, the simulations reveal intermediate species, providing valuable insights into the early stages of calcium carbonate formation. As a part of future work, Reactive MD simulations will be extended to tricalcium aluminate to further elucidate cement carbonation mechanisms. The computational framework developed here establishes a foundation for ongoing research into cement hydration and carbonation, offering a mechanistic understanding that supports the design of sustainable, low-carbon construction materials.

## 2. Abbreviations and acronyms

Abbreviation / Acronym	Description
C <sub>3</sub> S	Tricalcium Silicate
C <sub>3</sub> A	Tricalcium Aluminate
C <sub>2</sub> S	Dicalcium Silicate
CSI	Cement sustainability initiative
DFT	Density Functional Theory
ASE	Atomic Simulation Environment
MD	Molecular Dynamics
MSD	Mean Squared Displacement
PBE	Perdew-Burke-Ernzerhof
RDF	Radial Distribution Function
QE	Quantum Espresso

## 3. Background

The present document constitutes the Deliverable D1.1 "Benchmark of Carbonation Reaction Mechanisms of Clinker" in the framework of the Marie Sklodowska-Curie Actions Doctoral Network Project 101119715 – CONTRABASS as described in the HORIZON-MSCA-2022-DN-01.

The cement industry is the second-largest source of industrial CO<sub>2</sub> emissions, responsible for roughly 7% of global output. Reports from the International Energy Agency (IEA) and the Cement Sustainability Initiative (CSI) indicate that emissions from this sector could increase by another 4% by 2050, despite efforts to implement more sustainable practices (4). This poses a significant challenge to global efforts to cut greenhouse gas emissions and transition toward sustainable construction.

A major share of these emissions arises from clinker production, which involves the decomposition of limestone and other carbonate-rich materials. This process inevitably releases CO<sub>2</sub> as part of conventional cement chemistry. One mitigation strategy has been to reduce clinker content by partially or fully substituting it with alternative materials. However, this approach comes with limitations.

Over the years, researchers have explored various methods to reduce cement use,



including chemical admixtures, nanomaterials (e.g., graphene), fibre-reinforced polymers, zeolites, and supplementary cementitious materials such as fly ash and slag (5). Optimizing aggregate size and proportions has also shown benefits in some cases. Nevertheless, studies suggest that cement substitution can only cut CO<sub>2</sub> emissions by about 20% (3). Full replacement remains controversial, as hydrated Portland cement is essential for concrete's strength and durability. Furthermore, many alternatives are either scarce, costly, or pose challenges such as performance trade-offs or environmental impacts.

Despite these obstacles, cement and concrete remain indispensable to modern infrastructure, forming the backbone of roads, bridges, and buildings. Conventional Portland cement primarily consists of tricalcium silicate  $(C_3S)$  and dicalcium silicate  $(C_2S)$ , which account for about 80% of the binder (6). These phases require substantial limestone inputs and energy-intensive heating, resulting in significant  $CO_2$  emissions.

In recent years, mineral carbonation has emerged as a promising pathway for emission reduction in cement systems (7). This process involves reacting CO<sub>2</sub> with calcium-bearing phases in cement to form stable calcium carbonate. Although natural carbonation occurs slowly over a structure's lifespan, research has increasingly focused on accelerating carbonation during early curing or even after demolition. Accelerated carbonation has shown potential benefits, including enhanced impermeability and reduced corrosion of steel reinforcement (4).

However, carbonation in cement is complex. Hydrated cement contains multiple phases that react with CO<sub>2</sub> at different rates. Calcium silicate hydrates and portlandite carbonate relatively quickly, while calcium aluminates react more slowly or may remain unreactive under standard conditions (8). This heterogeneity makes carbonation outcomes difficult to predict and control in practice.

To better understand potential cement carbonation mechanisms, we performed Reactive MD simulations using the ReaxFF force fields developed by Adri van Duin and collaborators. These simulations focused on the interactions of CO<sub>2</sub>–rich fluids with C<sub>3</sub>S, providing atomic-scale insights into carbonation reactions (9).

## 4. Objective/Aim

This document has been prepared to provide insights into the mechanisms of CO<sub>2</sub> mineralisation in cement systems. It investigates how clinker phases interact with CO<sub>2</sub> at



the atomic scale using Reactive MD simulations, focusing on reaction pathways, energy barriers, and the influence of environmental factors on carbonation efficiency. The overarching goal is to advance the development of low-emission cement technologies and contribute to the broader transition toward sustainable construction materials.

#### 5. Content of the deliverable

## 5.1. Simulation Methodology

# 5.1.1. First-Principles Relaxation of C3S Using Density Functional Theory

Before conducting dynamic simulations, the solid C3S phase was structurally optimized using density functional theory (DFT) to remove residual stress, internal distortions, and artificial geometric artifacts. These calculations were performed with the *Quantum ESPRESSO* code, which employs a plane-wave pseudopotential formalism (6). The objective was to ensure that subsequent Reactive MD simulations started from a fully relaxed, zero-stress alite substrate.

The PBE (Perdew–Burke–Ernzerhof) generalized gradient approximation (10) was used to describe exchange–correlation energy, with Grimme's D2 van der Waals correction (11) added to account for long-range dispersion interactions. Variable-cell relaxation (vc-relax) allowed both lattice vectors and atomic positions to relax simultaneously, capturing anisotropic strain responses in C3S (12).

Electron–ion interactions were modeled with ultrasoft and PAW pseudopotentials (13) from the *Quantum ESPRESSO* library. A plane-wave cutoff of 80 Ry ensured energy and force convergence within 1 meV/atom. Brillouin zone sampling employed a  $2 \times 2 \times 2$  Monkhorst–Pack grid (14). Electronic minimization used Davidson diagonalization (15) with tuned mixing parameters to avoid charge sloshing. Convergence thresholds were set to  $10^{-8}$  Ry for total energy and  $10^{-4}$  Ry/Bohr³ for pressure. Up to 500 ionic steps were allowed, with full relaxation of all atoms and lattice vectors at each step.

The final structure exhibited no residual stress and bond lengths/angles consistent with crystallographic data. This relaxed configuration was exported as the substrate for subsequent Reactive MD simulations using ReaxFF force fields (16).

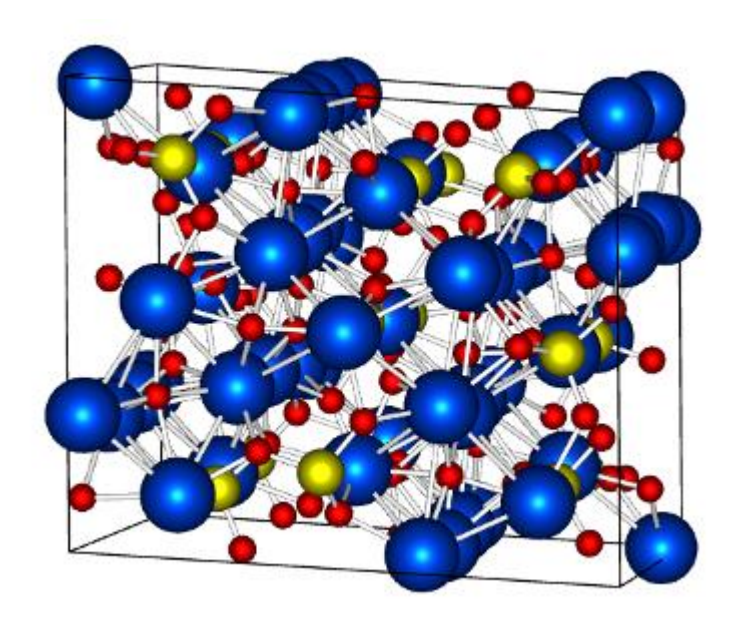


Figure 1. Structure of the C<sub>3</sub>S unit cell after first-principles relaxation using DFT

#### 5.1.2. Hydration of C3S

#### a. Construction of the C<sub>3</sub>S-Water Atomistic Model

To study molecular-level hydration of C<sub>3</sub>S (tricalcium silicate or also known as alite), we constructed an atomistic model of a solid–liquid interface. The goal was to simulate the interaction of water with an alite surface under early-stage cement hydration conditions.

The DFT-relaxed alite unit cell was first transformed from its triclinic representation into a cubic form using the Atomic Simulation Environment (ASE), simplifying periodic boundary conditions while preserving local atomic environments. A  $2 \times 2 \times 2$  supercell was then generated, providing sufficient surface area and bulk-like interior. To accommodate a water slab, the z-dimension was extended by 37.2 Å, introducing a vacuum gap.

A water layer was built using a grid-based placement algorithm. Each molecule had a 0.9584 Å O–H bond length and a 104.45° bond angle (10,17). Molecules were spaced 3.0 Å laterally and 2.75 Å vertically, with the first layer 2.5 Å above the highest oxygen atom on the alite surface. A total of 1,000 molecules formed a multilayer water slab with realistic density. Charges were initially set to zero, to be dynamically equilibrated during ReaxFF simulations.

## b. Reactive MD of Hydration with ReaxFF

Reactive MD simulations were carried out in LAMMPS using ReaxFF (18), which allows dynamic bond breaking and formation. Parameters merged Ca-O/H and Si-O/H



sets, enabling hydration processes such as water dissociation, surface hydroxylation, Ca leaching, and silicate depolymerization (19,20).

Charge equilibration was performed every timestep (tolerance 10<sup>-6</sup>, radius 10 Å, cutoff 2 Å) (21). Initial velocities were assigned from a Maxwell–Boltzmann distribution at 300 K. After conjugate gradient minimization, equilibration was performed in the NPT ensemble at 300 K and 1 atm using a Nosé–Hoover thermostat/barostat (22) (relaxation time 50 fs) w(23). The timestep was 0.2 fs to ensure stability in hydrogen-bonded reactions (24).

Simulations ran for 10 ns. Thermodynamic data, e.g., temperature, pressure, and both kinetic and potential energies, were logged every 1,000 steps, and atomic configurations were dumped at the same frequency for post-analysis.

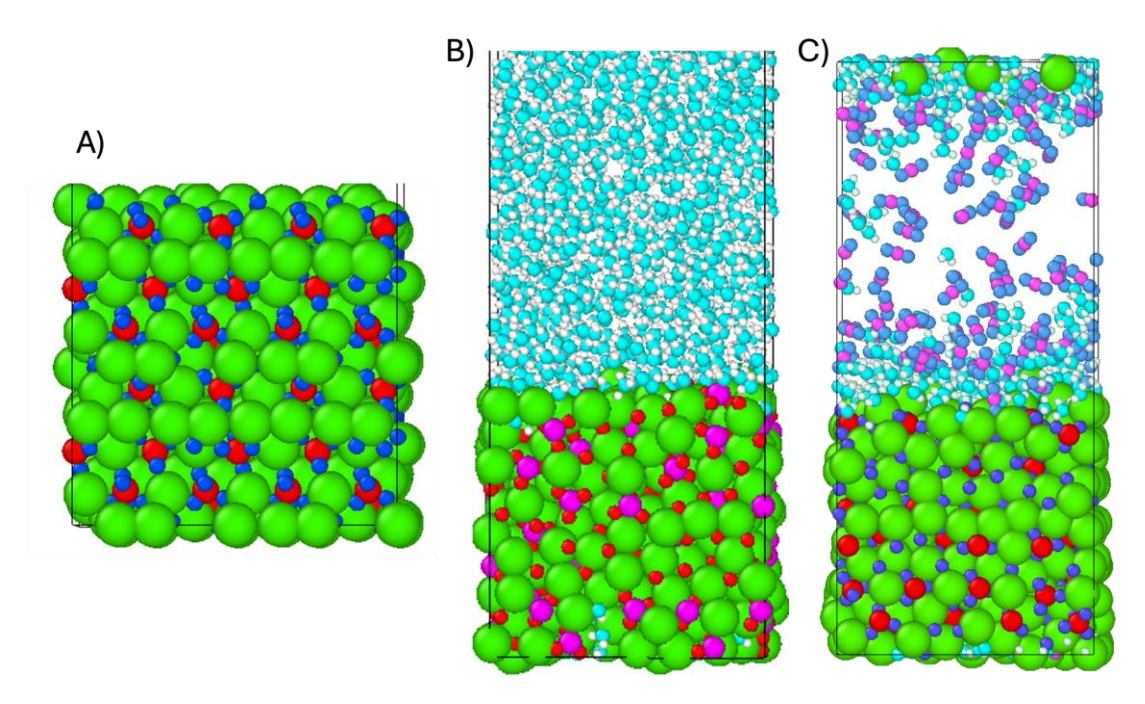


**Figure 2.** (A) Crystal structure of tricalcium silicate. Simulation snapshots of thin-film configurations of (B) H<sub>2</sub>O and (C) CO<sub>2</sub>—H<sub>2</sub>O mixtures on tricalcium silicate surfaces.

#### 5.1.3. Carbonation of C3S

#### a. Construction of the Atomistic Carbonation Model

For carbonation, a hybrid solid–liquid–gas model was built. The pre-relaxed alite supercell (2´2´2, elongated by 37.2 Å along the Z direction) was combined with explicit water and CO<sub>2</sub> molecules. Placement used a Python script with ASE and NumPy. Water molecules had 0.9584 Å O–H bonds and a 104.45° bond angle; CO<sub>2</sub> molecules were linear

with standard bond lengths. A placement algorithm ensured minimum separations: 2.8 Å (O–O in water), 3.2 Å (C–C in CO<sub>2</sub>), 3.0 Å (mixed species), and 2.5 Å clearance above C<sub>3</sub>S. Layers were spaced 2.75 Å (water) and 3.0 Å (CO<sub>2</sub>), with 1.5 Å separation between species. The system, consisting of 335 water molecules and 114 CO<sub>2</sub> molecules (molar ratio ~2.9:1), was used to initialize the simulation. At later stages, the simulation box will be further saturated with carbonate and bicarbonate ions to capture the pH-dependent behavior of cement carbonation.

#### b. Reactive MD of C3S Carbonation

Carbonation simulations were conducted in LAMMPS using ReaxFF parameters developed for metal carbonates in aqueous solution by Van Duin et al. (25). This force field models hydration, carbonation, and calcium carbonate precipitation. The energy and force cutoff tolerance value was set at  $1.0 \times 10^{-5}$  kcal mol<sup>-1</sup>. The low and high taper radius values in the force field were 0.0 and 10.0, respectively. The charge equilibration precision was  $1.0 \times 10^{-6}$ . Periodic boundary conditions were applied in all directions (26).

The simulation protocol followed a sequential, multi-stage workflow. First, the structure was energy-minimized using the conjugate gradient method with convergence thresholds of 1×10<sup>-5</sup> for both energy and force (27). This step relieved local stresses and eliminated high-energy overlaps from molecule placement. After minimization, the system was equilibrated in the canonical (NVT) ensemble at 298 K for 500,000 timesteps (100 ps), using a Nosé-Hoover thermostat (22) with a 100 fs damping constant to maintain thermal stability. Subsequently, pressure equilibration was performed in two stages under the isothermal-isobaric (NPT) ensemble. The initial stage lasted 10,000 timesteps (2 ps) to initiate pressure relaxation, followed by a production phase of 20,000,000 timesteps (2.4 ns) with a 0.2 fs timestep, allowing accurate capture of surface reactions involving silicates and calcium species. Simulation outputs were systematically managed. Thermodynamic quantities (temperature, pressure, potential, kinetic, and total energy, volume, and cell dimensions) were recorded every 1,000 steps. Atomic configurations were saved every 50,000 timesteps for detailed structural and reactive event analysis. Restart files containing the full system state were generated every 100,000 steps to ensure recovery and continuation capability.

Key phenomena observed included CO<sub>2</sub> dissolution, carbonic acid formation, calcium ion precipitation as calcium carbonate, surface restructuring, and silicate framework disruption. Hydration and carbonation proceeded concurrently, producing mixed-phase regions resembling real cementitious systems. The framework successfully captured both fast surface reactions and slower diffusion-controlled processes, offering insights into durability and optimization of cement carbonation resistance.

## 5.2. Summary of activities and research findings

#### 5.2.1. Analysis of the Structural Properties

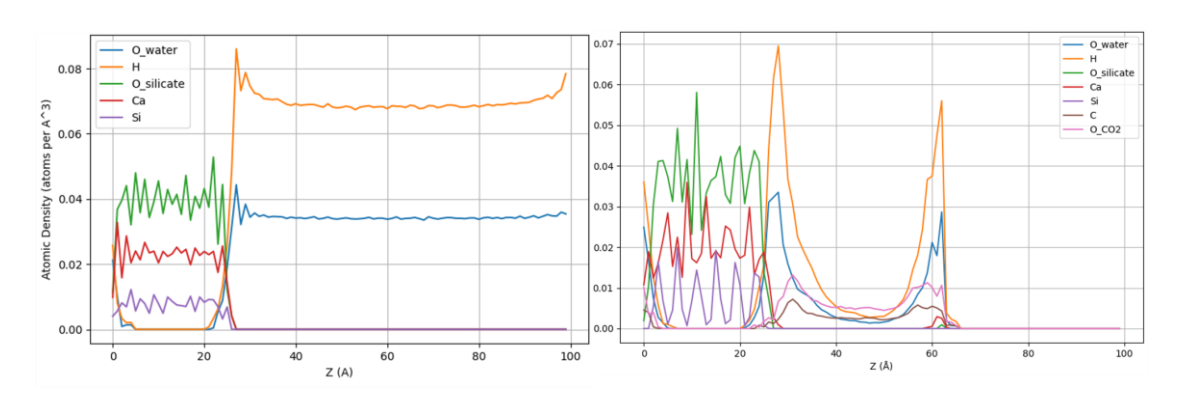


**Figure 3.** Atomic density profiles of  $CO_2$  carbon (C),  $CO_2$  oxygen (O\_CO<sub>2</sub>), water oxygen (O\_water), water hydrogen (H), calcium (Ca), silicon (Si), and C<sub>3</sub>S oxygen (O\_silicate) atoms along the Z direction for C<sub>3</sub>S surfaces during hydration (left panel) and carbonation (right panel). The reference (Z = 0) is defined as the average position of the bottom-layer atoms of C<sub>3</sub>S slab.

In Figure 3 (left panel), the atomic density profile provides insight into the organization of species within the tricalcium silicate (C<sub>3</sub>S)–water system. The z-axis represents the dimension normal to the C<sub>3</sub>S slab, separating the solid phase at the bottom from the liquid phase above. Between 0 and ~25 Å, the slab is characterized by the densities of calcium (Ca), silicate oxygen (O\_silicate), and silicon (Si), which display flat, consistent profiles, indicating a stable, well-ordered solid surface without significant restructuring during the simulation.

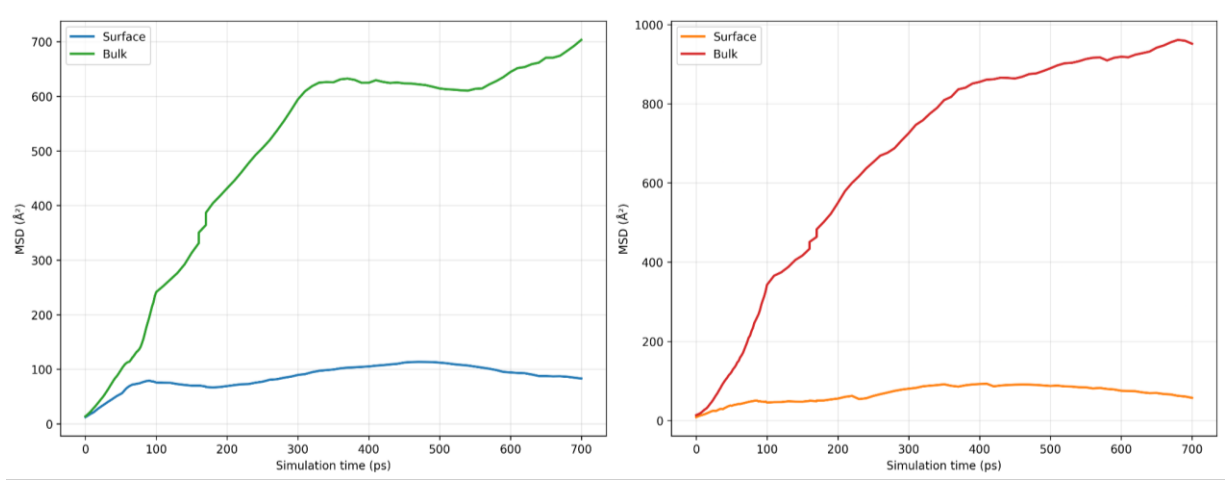
Above the surface, the densities of water oxygen (O\_water) and hydrogen (H) rise sharply from ~25 Å. The hydrogen density remains higher due to the 2:1 H/O ratio in water molecules. A distinct O\_water peak immediately beyond the surface signifies a structured first hydration layer. This interfacial layer is critical for early hydration processes such as water dissociation, Ca²+\_OH⁻ coordination, and the initial formation of calcium—silicate—hydrate (C-S-H) gel. Beyond ~30 Å, the O\_water and H profiles flatten, reflecting a homogeneous bulk liquid phase that sustains ion migration and reaction dynamics. This profile serves as a reference for hydration-driven reactions and highlights how interfacial water structuring provides the reactive environment consistent with known C₃S hydration mechanisms.

Figure 3 (right panel) shows the density profile under carbonation conditions. As in the hydration case, the slab extends up to ~25 Å, with Ca, O\_silicate, and Si densities



confirming structural preservation of the solid. However, key differences emerge above the surface. O\_water and H again spike, forming a hydration layer, though their structuring is modified by dissolved CO<sub>2</sub>. Notably, the densities of carbon (C) and CO<sub>2</sub> oxygen (O\_CO<sub>2</sub>) rise between ~30 and 60 Å, overlapping with the hydration layer. This region represents the main reactive interface where carbonation occurs. The spatial coexistence of carbon and calcium supports the formation of carbonation products via reactions between dissolved CO<sub>2</sub> and surface or solvated calcium ions.

#### 5.2.2. Analysis of the Dynamical Properties



**Figure 4.** Mean square displacement as a function of time for water (left panel) and CO<sub>2</sub> (right panel) molecules on the C<sub>3</sub>S surface, shown along the XY (surface) and XYZ (bulk) directions.

The mean squared displacement (MSD) is a fundamental statistical measure in molecular dynamics simulations used to quantify particle mobility over time. It describes how far, on average, a molecule or atom moves from its initial position as the system evolves. Mathematically, MSD is defined as (26)

$$MSD(t) = \langle |r_i(t) - r_i(0)|^2 \rangle$$

where  $r_i(t)$  is the position vector of the ith particle at time t, and the angle brackets denote averaging over all particles and time origins. In fluids, MSD is particularly important because it connects directly to the diffusion coefficient via the Einstein relation. In three dimensions, this relation is given by (26)

$$D = \frac{1}{6} \frac{d}{dt} MSD(t)$$

Thus, MSD not only describes molecular mobility but also provides an indirect measure of how confinement, surface chemistry, and intermolecular forces influence transport properties.

In this study, MSD calculations were performed to examine the dynamics of water and CO<sub>2</sub> in MD simulations of C<sub>3</sub>S interacting with aqueous and gaseous phases. For each species, two environments were analyzed: molecules in the bulk phase (unconfined) and molecules directly interacting with the C<sub>3</sub>S surface. This distinction is critical in cement chemistry, where hydration and carbonation are controlled by molecular mobility at mineral interfaces.

The MSD data in Figure 4 show the time evolution of displacements over a 700 ps simulation. For water, a strong contrast emerges between bulk and surface environments. Bulk water molecules (green dashed line) exhibit a steep increase in MSD, reaching ~700 Ų, consistent with classical Fickian diffusion in a homogeneous liquid. By contrast, water molecules at the C₃S surface show suppressed MSD values of ~100 Ų with a flattened trajectory, reflecting confinement and reduced mobility. This restriction likely arises from strong electrostatic interactions, hydrogen bonding with surface hydroxyl groups, or partial immobilization in calcium-rich regions of the surface. CO₂ shows a similar trend. Bulk CO₂ molecules diffuse more rapidly than water, surpassing 950 Ų by the end of the simulation—consistent with their smaller size and absence of hydrogen bonding. Near the C₃S surface, however, CO₂ mobility is drastically reduced, with MSD values plateauing below 80 Ų. This behavior suggests physisorption or transient trapping at the surface, where weak van der Waals or electrostatic interactions hinder diffusion despite the absence of strong chemical bonding.

Overall, the MSD analysis highlights the significant impact of surface adsorption on molecular mobility. Both water and CO<sub>2</sub> exhibit severe mobility restrictions at the C<sub>3</sub>S interface compared to their bulk behavior. Such immobilization is highly relevant to cement hydration and carbonation, as molecular diffusion governs the rate and spatial extent of reactions. Reduced mobility at the surface may delay reaction kinetics, produce heterogeneous reaction fronts, and influence long-term cement durability by altering porosity and ion transport pathways. These findings provide a foundation for further investigation. Future work will include quantitative estimation of diffusion coefficients through linear fitting of bulk MSD curves and the application of sub-diffusive models to more accurately capture interfacial dynamics. Published field cycling NMR experiments confirm that the time taken for a bound water molecule to migrate to a neighbouring site is of order microseconds and that water desorbs from the surfaces at a similar rate. These



#### 5.2.3. Reactivity of CO2-H2O mixture with C3S

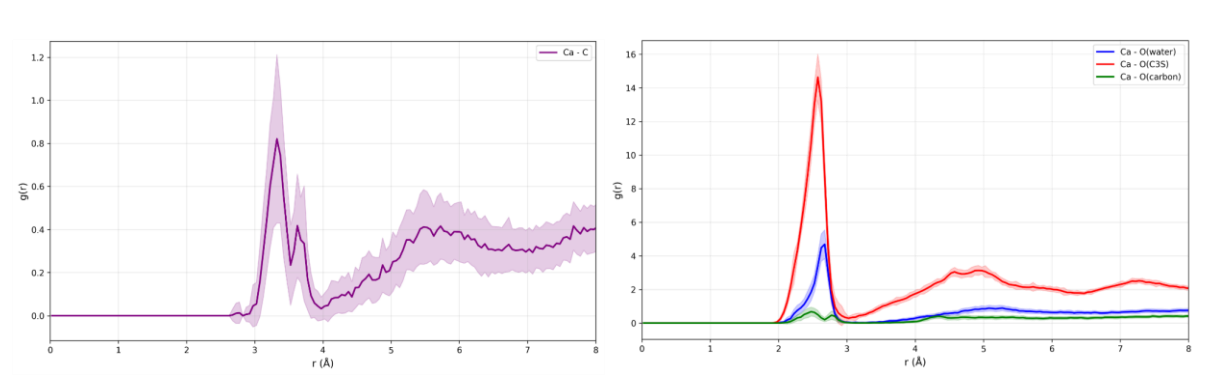


**Figure 5.** *Left*: Radial distribution functions of Ca–C<sub>CO2</sub> pair. *Right*: Radial distribution functions of Ca–O<sub>C3S</sub> (red), Ca–O<sub>H2O</sub> (blue), and Ca–O<sub>CO2</sub> (green) pairs.

The radial distribution function (RDF), g(r), is a key statistical measure in molecular dynamics that describes how atomic density varies with distance from a reference atom. It reflects the probability of finding a particle at a radial distance *r* relative to a random distribution at uniform density. In atomistic simulations of chemical processes such as C<sub>3</sub>S hydration and carbonation, RDF analysis provides valuable insights into evolving coordination environments (29). Here, RDFs are calculated between calcium atoms and selected neighboring atoms, e.g., carbon atoms from CO<sub>2</sub> molecules, oxygen atoms originating from water, CO<sub>2</sub> molecules, and the C<sub>3</sub>S lattice, in order to probe structural changes associated with carbonation and the evolution of calcium's local environment.

In Figure 5, left panel, the results show that the Ca–C<sub>CO2</sub> RDF exhibits a distinct first coordination peak near 3.3-3.4 Å, indicative of spatial associations between Ca atoms and carbon atoms of carbon dioxide. This distance is characteristic of carbonate-like interactions, signaling the early stages of Ca–CO<sub>3</sub> clustering (17). Although the peak intensity (g(r)  $\approx 0.8$ ) is modest compared to crystalline solids, its presence confirms that dissolved CO<sub>2</sub>-derived carbon atoms preferentially localize near calcium centers. A weaker second peak at  $\sim 3.7-3.8$  Å, together with a gradual rise beyond 4 Å, reflects the presence of more weakly associated carbon species—likely unreacted CO<sub>2</sub> molecules diffusing in the solvent but not yet incorporated into stable coordination structures. Overall, the moderate Ca–C peak suggests that carbonation has been initiated but remains highly dynamic.

To further characterize calcium's coordination, RDFs with oxygen atoms from different origins were analyzed. The Ca-O RDF for oxygen atoms in the C $_3$ S lattice shows a sharp first peak at  $\sim$ 2.4 Å with a height exceeding 14, consistent with strong ionic coordination in

the crystalline phase (17). This dominant signal highlights the structural persistence of C<sub>3</sub>S during the early stages of carbonation, with much of the calcium remaining embedded in the original lattice framework.

By contrast, the Ca–O RDF for water oxygen atoms exhibits a broader peak centered around 2.5 Å with a lower intensity (~5). This reflects partial solvation of calcium by water molecules at the surface, consistent with hydrated calcium environments observed in experiments and simulations. Such hydration is a prerequisite for carbonation, as calcium must be exposed to the aqueous phase to react with dissolved CO<sub>2</sub> (27).

Finally, the Ca–O RDF for oxygen from carbon-containing species reveals a modest but distinct peak at 2.6-2.7 Å (g(r)  $\approx$  1). Although weaker than the lattice or water signals, this peak confirms that carbonation has been initiated, with some calcium ions forming transient bonds to oxygen atoms of  $CO_2$  molecules. These interactions likely correspond to monodentate or bidentate carbonate coordination at the surface or near partially dissolved calcium sites. The relatively low intensity suggests that only a fraction of calcium has reacted at this stage and that carbonate species remain mobile and weakly stabilized.

Taken together, the RDF analysis reveals the coexistence of hydration and carbonation processes in the C<sub>3</sub>S-water-CO<sub>2</sub> system. The dominant Ca-O signal from the silicate lattice underscores the structural resilience of the solid phase, while the emerging Ca-O(water) and Ca-C peaks highlight the competition for calcium coordination between hydration and carbonation. The incorporation of CO<sub>2</sub> oxygen atoms into calcium's first coordination shell is a critical indicator of early carbonation, confirming the chemical accessibility of calcium and the simulation's ability to capture atomistic precursors of carbonate formation. Importantly, the results emphasize water's dual role—as both a hydration medium and a facilitator of carbonation through calcium solvation and mobilization (30).

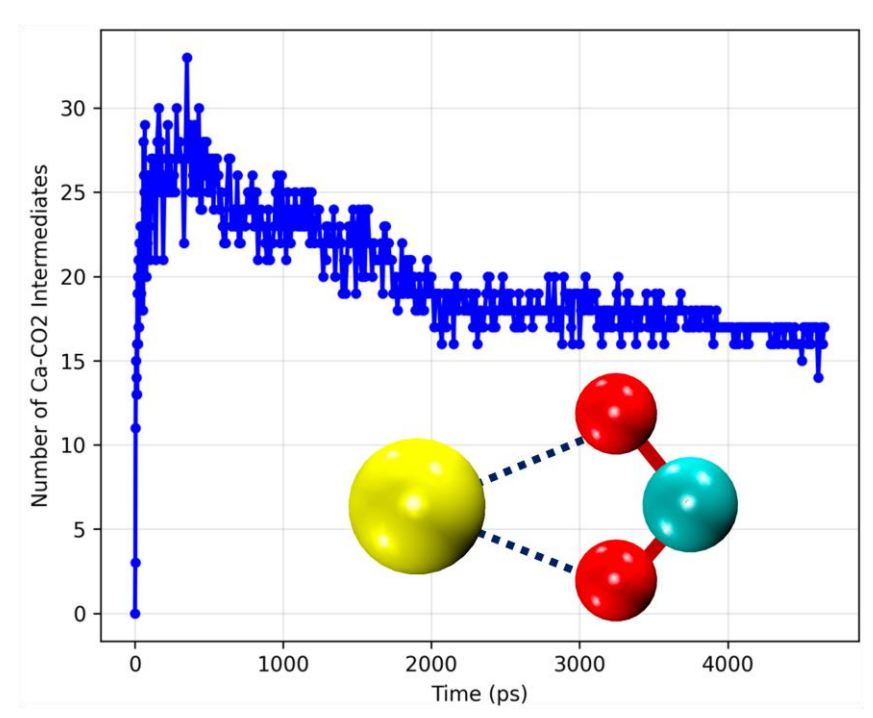


**Figure 6.** Evolution of Ca–O–C–O intermediates over time. Yellow, cyan, and red spheres represent calcium, carbon, and oxygen atoms from CO<sub>2</sub> molecules, respectively.

The kinetics of the carbonation process were monitored by tracking the number of bonds formed between calcium atoms and oxygen atoms from CO<sub>2</sub> molecules during the 4.8 ns simulation. Figure 6 presents the evolution of Ca–O–C–O intermediates over time. The reaction begins with a sharp increase in bond formation, rising from zero to 30 within 200 ps, indicative of an explosive initial reaction rate. This aligns with the MSD analysis, which showed that CO<sub>2</sub> molecules arriving at the C<sub>3</sub>S surface were rapidly immobilized. Following this rapid onset, the system enters a relaxation stage, during which the initial precipitate—likely disordered and high in energy—reorganizes into a more stable structure. After ~2 ns, the reaction rate slows as the early products form an amorphous layer on the C<sub>3</sub>S surface that hinders further access of CO<sub>2</sub> and water molecules.

To gain deeper insight, we analyzed the number of atoms involved in Ca–O–C–O intermediate species (Figure 7). The left panel shows the number of Ca and C atoms simultaneously engaged in intermediate formation. The red curve (Ca) remains consistently above the black curve (C), indicating greater participation of Ca atoms compared with C atoms. The gap between the curves suggests that oxygen atoms from CO<sub>2</sub> frequently coordinate with multiple Ca atoms. To validate this, we quantified nucleation species (right panel of Figure 7). The results show that species in which a single oxygen bridges two calcium atoms form rapidly at the outset but decline to ~12 after 2 ns,

suggesting that such double bridges form easily but are reduced as the precipitate undergoes structural reorganization. We also observe the transient formation of species where one oxygen atom coordinates with three calcium atoms, but not with four.

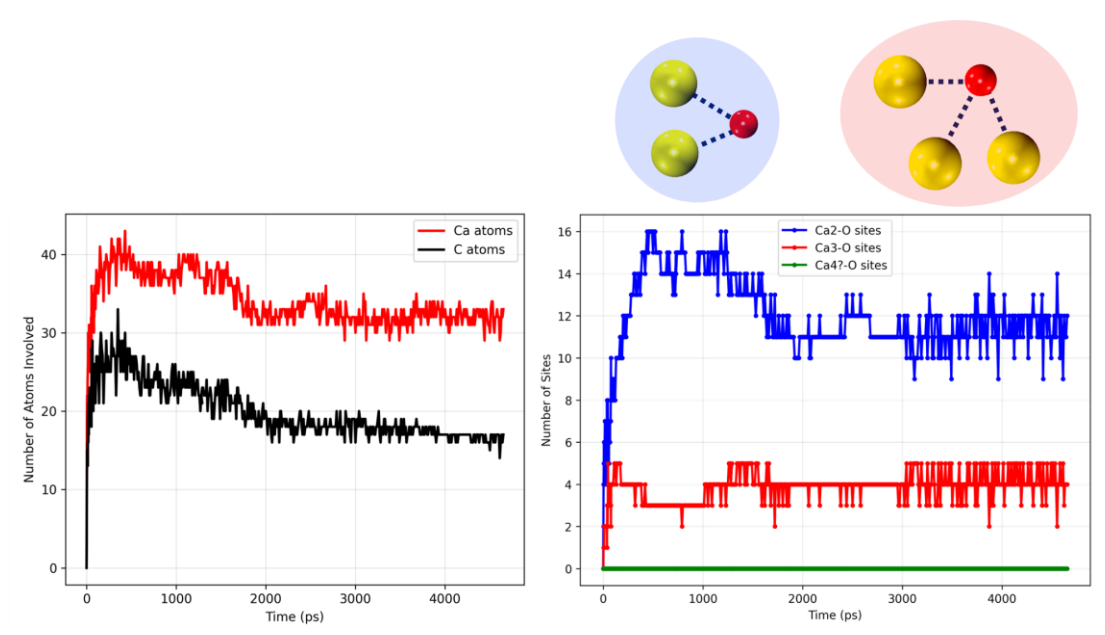


**Figure 7.** Left: Evolution of the number of Ca and C atoms participating in Ca–O–C–O intermediate formation as a function of time. Right: Evolution of the number of species in which a CO<sub>2</sub> oxygen atom is bonded to two (blue) or three (red) calcium atoms.

#### 6. Conclusions and Future Works

The primary source of carbon dioxide (CO<sub>2</sub>) emissions in cement production is the calcination of limestone, a process that releases over one ton of CO<sub>2</sub> per ton of cement. Since plant upgrades alone cannot eliminate these emissions, reducing the environmental impact of concrete is critical. Carbon Capture and Utilization (CCU) offers a promising pathway to develop carbon-neutral cement and concrete. This study employs Reactive MD simulations to examine the carbonation curing process of clinker phases, e.g., tricalcium silicate (C<sub>3</sub>S). Using advanced computational modeling, we investigate the atomic-scale structure, reaction kinetics, and thermodynamics of C<sub>3</sub>S during carbonation. The radial distribution function (RDF) analysis of atom pairs reveals the onset of cement carbonation, with the first RDF peaks for Ca–O<sub>water/CO2</sub> and Ca–C<sub>CO2</sub> at 0.24 nm and 0.34 nm, respectively, aligning with the structure of calcium carbonate and confirming carbonation product formation. The simulations also reveal intermediate species, offering key insights into the early stages of calcium carbonate formation. The process can be accelerated by

introducing carbonate and bicarbonate ions into the solution at later stages. To capture the time-dependent sequence of cement hydration and carbonation, we will analyze the evolution of Ca–OH, Ca–O–C–O, and other intermediate species identified in this study as a function of time. This will provide a clearer understanding of the hydration prerequisites for cement carbonation.

Building on the initial setup and preliminary analysis of carbonation in C<sub>3</sub>S using the ReaxFF force field, the next stages of this research will extend to exploring carbonation mechanisms in both dicalcium silicates and tricalcium aluminates. While the RDFs and mean squared displacements (MSDs) have provided early insights into atomic structure and mobility, a more detailed structural and chemical characterization will be carried out. This will involve tracking the formation and evolution of carbonate species, as well as identifying hydration products and their transformations during carbonation. In addition, we will quantify the coordination environments and reaction dynamics of key species, including calcium ions, CO<sub>2</sub>, and H<sub>2</sub>O.

Future simulations will incorporate environmental conditions relevant to practical curing, such as varying CO<sub>2</sub> partial pressures, humidity levels, and solution ionic strengths, in order to predict and optimize carbonation efficiency in next-generation calcium carbonate cements (CCCs). A parallel ReaxFF-based workflow will be developed for tricalcium aluminate to investigate why carbonation is markedly less significant in aluminate phases.

To complement the ReaxFF approach, AIMD and metadynamics simulations will be employed for selected reaction events. These advanced methods will validate pathways identified in ReaxFF simulations, characterize transition states and intermediate species, and provide accurate activation energy barriers for key reactions involving CO<sub>2</sub>, calcium ions, and hydroxyl groups.

#### 7. References

- 1. GLOBAL CEMENT AND CONCRETE INDUSTRY ANNOUNCES ROADMAP TO ACHIEVE GROUNDBREAKING 'NET ZERO' CO2 EMISSIONS BY 2050: GCCA [Internet]. [cited 2025 Sept 11]. Available from: https://gccassociation.org/news/global-cement-and-concrete-industry-announces-roadmap-to-achieve-groundbreaking-net-zero-co2-emissions-by-2050/?utm\_source=chatgpt.com
- 2. Andersson R, Stripple H, Gustafsson T, Ljungkrantz C. Carbonation as a method to improve climate performance for cement based material. Cem Concr Res. 2019 Oct;124:105819.



- 3. Flower DJM, Sanjayan JG. Green house gas emissions due to concrete manufacture. Int J Life Cycle Assess. 2007 July;12(5):282–8.
- 4. Berger RL, Young JF, Leung K. Acceleration of hydration of calcium silicates by carbon dioxide treatment. Nat Phys Sci. 1972;240(97):16–8.
- 5. Blezard RG. The history of calcareous cements. Leas Chem Cem Concr. 1998;1–32.
- 6. Barbosa W, Honorio T. Triclinic tricalcium silicate: Structure and thermoelastic properties from molecular simulations. Cem Concr Res. 2022 Aug;158:106810.
- 7. Boumaaza M, Turcry P, Huet B, Aït-Mokhtar A. Influence of carbonation on the microstructure and the gas diffusivity of hardened cement pastes. Constr Build Mater. 2020 Aug;253:119227.
- 8. Ming X, Si W, Yu Q, Sun Z, Qiu G, Cao M, et al. Molecular insight into the initial hydration of tricalcium aluminate. Nat Commun. 2024 Apr 4;15(1):2929.
- 9. Senftle TP, Hong S, Islam MM, Kylasa SB, Zheng Y, Shin YK, et al. The ReaxFF reactive force-field: development, applications and future directions. Npj Comput Mater. 2016 Mar 4;2(1):15011.
- 10. Corongiu G, Clementi E. Water Structure from Computational Chemistry. In: Wipff G, editor. Computational Approaches in Supramolecular Chemistry [Internet]. Dordrecht: Springer Netherlands; 1994 [cited 2025 Sept 11]. p. 1–29. Available from: https://doi.org/10.1007/978-94-011-1058-7\_1
- 11. Grimme S. Semiempirical GGA-type density functional constructed with a long-range dispersion correction. J Comput Chem. 2006;27(15):1787–99.
- 12. Xie H, Jiang W, Hou Z, Xue Y, Wang Y, Liu T, et al. DFT study of the carbonation on mineral aerosol surface models of olivine: effect of water. Environ Earth Sci. 2017 Nov;76(21):732.
- 13. Perdew JP, Burke K, Ernzerhof M. Generalized Gradient Approximation Made Simple. Phys Rev Lett. 1996 Oct 28;77(18):3865–8.
- 14. Monkhorst HJ, Pack JD. Special points for Brillouin-zone integrations. Phys Rev B. 1976 June 15;13(12):5188–92.
- 15. Davidson ER. The iterative calculation of a few of the lowest eigenvalues and corresponding eigenvectors of large real-symmetric matrices. J Comput Phys. 1975 Jan 1;17(1):87–94.
- 16. van Duin ACT, Dasgupta S, Lorant F, Goddard WA. ReaxFF: A Reactive Force Field



- for Hydrocarbons. J Phys Chem A. 2001 Oct 1;105(41):9396-409.
- 17. Dunstetter F, De Noirfontaine MN, Courtial M. Polymorphism of tricalcium silicate, the major compound of Portland cement clinker. Cem Concr Res. 2006 Jan;36(1):39–53.
- 18. Plimpton S. Fast Parallel Algorithms for Short-Range Molecular Dynamics. J Comput Phys. 1995 Mar 1;117(1):1–19.
- 19. Manzano H, Pellenq RJM, Ulm FJ, Buehler MJ, van Duin ACT. Hydration of Calcium Oxide Surface Predicted by Reactive Force Field Molecular Dynamics. Langmuir. 2012 Mar 6;28(9):4187–97.
- 20. Larsson HR, Duin ACT van, Hartke B. Global optimization of parameters in the reactive force field ReaxFF for SiOH. J Comput Chem. 2013 Sept 30;34(25):2178–89.
- 21. Rappe AK, Goddard WA. Charge equilibration for molecular dynamics simulations. J Phys Chem. 1991 Apr;95(8):3358–63.
- 22. Nosé S. A unified formulation of the constant temperature molecular dynamics methods. J Chem Phys. 1984 July 1;81(1):511–9.
- 23. (PDF) Canonical Dynamics: Equilibrium Phase-Space Distributions. ResearchGate [Internet]. 2025 Aug 6 [cited 2025 Sept 11]; Available from: https://www.researchgate.net/publication/287996327\_Canonical\_Dynamics\_Equilibrium\_Phase-Space\_Distributions
- 24. Manzano H, Durgun E, López-Arbeloa I, Grossman JC. Insight on Tricalcium Silicate Hydration and Dissolution Mechanism from Molecular Simulations. ACS Appl Mater Interfaces. 2015 July 15;7(27):14726–33.
- 25. Gale JD, Raiteri P, Duin ACT van. A reactive force field for aqueous-calcium carbonate systems. Phys Chem Chem Phys. 2011 Sept 6;13(37):16666–79.
- 26. Allen MP, Tildesley DJ. Computer simulation of liquids. Second edition. Oxford, United Kingdom: Oxford University Press; 2017. 626 p.
- 27. Rani RS, Saharay M. Molecular dynamics simulation of protein-mediated biomineralization of amorphous calcium carbonate. RSC Adv. 2019;9(3):1653–63.
- 28. Korb JP. Nuclear magnetic relaxation of liquids in porous media. New J. Phys. 2011; 13: 035016.
- 29. Dongshuai H, Zeyu L, Peng Z, Qingjun D. Molecular structure and dynamics of an aqueous sodium chloride solution in nano-pores between portlandite surfaces: a molecular dynamics study. Phys Chem Chem Phys. 2016;18(3):2059–69.



30. Salah Uddin KM, Izadifar M, Ukrainczyk N, Koenders E, Middendorf B. Dissolution of  $\beta$ -C2S Cement Clinker: Part 1 Molecular Dynamics (MD) Approach for Different Crystal Facets. Materials. 2022 Sept 14;15(18):6388.